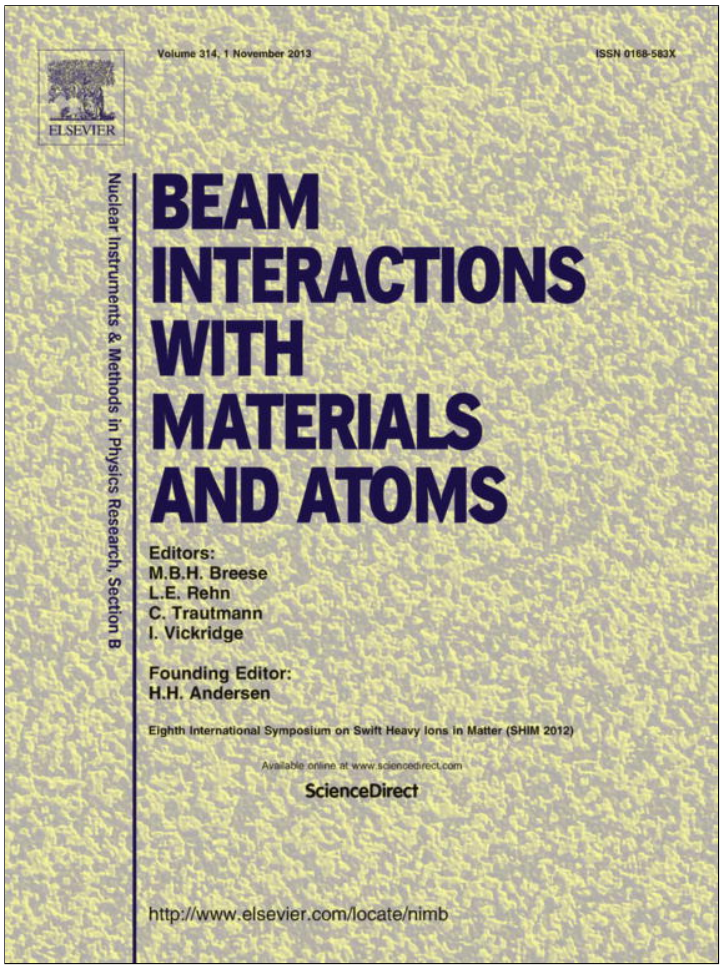

Nuclear Instruments and Methods in Physics Research B 314 (2013) 66–70

Contents lists available at SciVerse ScienceDirect

Nuclear Instruments and Methods in Physics Research B

journal homepage: www.elsevier.com/locate/nimb

Proton-induced ionization of isolated uracil molecules: A theory/experiment confrontation

C. Champion [a,*], M.E. Galassi [b], P.F. Weck [c], S. Incerti [a], R.D. Rivarola [b], O. Fojón [b], J. Hanssen [d], Y. Iriki [e], A. Itoh [e]

[a] Université Bordeaux 1, CNRS/IN2P3, Centre d'Etudes Nucléaires de Bordeaux-Gradignan, CENBG, France
[b] Instituto de Física Rosario, CONICET and Universidad Nacional de Rosario, Argentina
[c] Department of Chemistry and Harry Reid Center for Environmental Studies, University of Nevada Las Vegas, USA
[d] Laboratoire de Physique Moléculaire et des Collisions, UMR CNRS 7565, Université de Lorraine, France
[e] Department of Nuclear Engineering, Kyoto University, Kyoto 606-8501, Japan

ARTICLE INFO

Article history:
Received 30 November 2012
Received in revised form 5 March 2013
Accepted 15 April 2013
Available online 18 June 2013

Keywords:
Ionization
Cross sections
Protons
RNA-uracil

ABSTRACT

Proton-induced ionization of RNA-uracil target is here theoretically described by two quantum-mechanical models, namely, a first perturbative one developed within the 1st Born approximation and a second one based on the continuum distorted wave approximation. Comparisons between theory and experiments are reported in terms of differential as well as total cross sections exhibiting a very good agreement for the kinematics here investigated.

1. Introduction

In view of their potential applications in diverse fields like radioprotection, radiobiology, medical imaging and even radiotherapy for treatment planning, numerical codes of charged particle transport – generally based on Monte Carlo techniques – have been extensively developed to simulate the particle-matter interactions occurring along the so-called post-irradiation "physical stage".

In spite of the fact that there is nowadays an increasing activity around the development of simulation codes able to tackle radio-induced damages, several questions are still today unanswered and numerous challenges remain in the development of Monte Carlo charged-particle track structure simulation codes [1]. Among them, one important thought-provoking question is whether the use of water to simulate the biological medium (in which this molecule is present in the cellular environment for more than 60–70% in mass depending on the age of the patient), is valid or not.

In this context, we have recently developed a series of theoretical models to estimate the ionization and the electron capture cross sections for protons colliding with the different DNA/RNA components [2–4]. These models – based on either the 1st Born approximation with correct boundary conditions (CB1 model) or the continuum distorted wave-eikonal initial state approach (CDW-EIS model) – are detailed in the following. However, let us first here remind that the CB1 model describes the active (ejected) electron as being in bound and continuum states of the target field in the entry and exit channel, respectively, while in the CDW-EIS approximation, a more '*complete*' representation of the active electron is introduced, considering that it evolves in the simultaneous presence of the projectile and target fields in the entry and exit channels at all collision times, for single ionization as well as for single electron capture. In this way, CB1 is a one-centre model whereas CDW-EIS is a two-centre one. Besides, let us add that correct boundary conditions are considered in the present CB1 model, meaning that asymptotic Coulomb long-range interactions between the projectile and all the particles composing the target are accounted for in the initial and final wave functions. Finally, let us remind that the two present models are expected to be valid for high enough collision energies [9]. Indeed, the CDW-EIS model has been introduced to give a better description than the one-center models of both the ionization and the capture processes, in particular in the intermediate impact energy regime i.e. where the impact velocity is comparable to the initial electron orbital velocity.

Using these models, we have then successively investigated the case of the DNA/RNA bases, *i.e.* adenine, thymine, cytosine, guanine

* Corresponding author.
E-mail address: champion@cenbg.in2p3.fr (C. Champion).

0168-583X/$ - see front matter © 2013 Elsevier B.V. All rights reserved.
http://dx.doi.org/10.1016/j.nimb.2013.04.063

and uracil (the latter replacing thymine in the single-stranded ribonucleic acid RNA during DNA transcription due to its efficient base pairing with adenine through the formation of hydrogen bonds). More recently, the sugar-phosphate backbone – which represents the main DNA constituent as it is involved in the strand break induction – has been studied.

The present work aims to compare the provided cross sections to a recent set of experimental results obtained by Itoh and coworkers at Kyoto University in continuation of their previous works on adenine [5,6].

Thus, in the sequel, we briefly report on the theoretical support of our theoretical models as well as the experimental set-up used for estimating the doubly- and singly-differential cross sections of uracil ionization. The theoretical predictions are then compared to the experimental data for a proton energy of 1 MeV and for ejected electron energies ranging from 1 eV to 1 keV and ejection angles covering a large range (15–165°).

2. The theoretical models

The main physical aspects of the CDW-EIS and CB1 models are exposed in the sequel.

2.1. Ionization CDW-EIS treatment

In the CDW-EIS model, the initial and final distorted wave functions are chosen as

$$\chi_\alpha^+ = \frac{\exp(i\boldsymbol{K}_\alpha.\boldsymbol{R})}{(2\pi)^{3/2}}\varphi_\alpha(\boldsymbol{x})\exp\left[-i\frac{Z_P}{v}\ln(vs+\boldsymbol{v}.\boldsymbol{s})\right] \tag{1}$$

and

$$\chi_\beta^- = \frac{\exp(i\boldsymbol{K}_\beta.\boldsymbol{R})}{(2\pi)^{3/2}}.\varphi_\beta(\boldsymbol{x})N^*(Z_T^*/k)\cdot{}_1F_1(-iZ_T^*/k;1;-ikx-i\boldsymbol{k}.\boldsymbol{x}) \times N^*(Z_P/p)\cdot{}_1F_1(-iZ_P/p;1;-ips-i\boldsymbol{p}.\boldsymbol{s}) \tag{2}$$

where the vectors $\boldsymbol{x}$ and $\boldsymbol{s}$ give the positions of the active electron with respect to the center of mass of the residual target and to the projectile, respectively, whereas $\boldsymbol{R}$ denotes the position of the projectile with respect to the center of mass of the target. Furthermore, $\boldsymbol{k}$ denotes the momentum of the ejected electron seen from the target, $\mathbf{p}=\mathbf{k}-\mathbf{v}$ the momentum of this electron with respect to the projectile, and $\mathbf{K}_\alpha$ and $\mathbf{K}_\beta$ the momenta of the reduced particle of the complete system in the entry and exit channels, respectively, Z_P being the projectile charge and Z_T^* an effective target charge. In Eq. (2), $N(a)=\exp(\pi a/2)\Gamma(1-ia)$ and $N^*(a)$ indicates the conjugate of $N(a)$.

The function $\varphi_\alpha(\mathbf{x})$ describes the bound electron orbital wave function and the multiplicative projectile eikonal phase in Eq. (1) (depending on the electronic coordinate $\boldsymbol{s}$ of the active electron) indicates that the active electron moves simultaneously in a bound state of the target and implicitly in a projectile eikonal continuum one. The eikonal form of the projectile-active electron continuum is chosen to preserve the normalization of the initial distorted wave function [10]. In the exit channel, $\varphi_\beta(\mathbf{x})$ is a plane wave that multiplied by the effective Coulomb continuum factor (see Eq. (2)) gives the continuum of the ionized electron in the field of the residual target. The inclusion of a multiplicative projectile continuum factor indicates that the electron is moving in a continuum state associated to the combined action of the residual target and the projectile fields, both considered on equal footing [11]. Thus, initial and final distorted wave functions in CDW-EIS are chosen as two-center ones in the sense that the active electron is considered under the simultaneous presence of the projectile and residual target potentials in the entry and exit channels at all distances between aggregates. In this way, the presence of disconnected diagrams associated with the separate consideration of these potentials, which could induce the presence of divergences in the corresponding Lippmann–Schwinger development [12,13], is avoided in CDW-EIS. Moreover, it includes in the initial and final distorted wave functions, the long range Coulomb character of the interaction of the active electron with the projectile in the entry channel and also with the residual target in the exit one, so they satisfy correct asymptotic conditions in both channels [14]. This property is crucial to avoid the presence of the divergent contribution of the intermediate elastic channel in the ionization reaction [15]. For more details on the distorted initial and final wave functions and the corresponding perturbation potentials, the interested reader is referred to [9].

2.2. Ionization CB1 treatment

In the CB1 model, which can be considered as an extension of the approximation introduced by Belkić et al. [16] for electron capture, the initial and final wave functions are chosen as

$$\phi_\alpha^+ = \frac{\exp(i\boldsymbol{K}_\alpha.\boldsymbol{R})}{(2\pi)^{3/2}}\varphi_\alpha(\boldsymbol{x})\exp\left[-i\frac{Z_P}{v}\ln(vR-\boldsymbol{v}.\boldsymbol{R})\right] \tag{3}$$

and

$$\phi_\beta^- = \frac{\exp(i\boldsymbol{K}_\beta.\boldsymbol{R})}{(2\pi)^{3/2}}\varphi_\beta(\boldsymbol{x})N^*(Z_T^*/k)\,{}_1F_1(-iZ_T^*/k;1;-ikx-i\boldsymbol{k}.\boldsymbol{x}) \times\exp\left[+i\frac{Z_P}{v}\ln(vR+\boldsymbol{v}.\boldsymbol{R})\right] \tag{4}$$

Let us note that the main difference between the initial wave function described by Eq. (3) and that given in the CDW-EIS approach resides in an eikonal phase depending on $\boldsymbol{R}$ instead of $\boldsymbol{s}$, so that the asymptotic boundary conditions associated with the projectile-active electron interaction are now preserved but ϕ_α^+ presents a one-target center character. In the exit channel (see Eq. (4)), an asymptotic version of this interaction is also considered (depending again on $\boldsymbol{R}$), which will be valid under the dynamic condition $k << v\ (x << R)$ [17]. So, in the CB1 approximation for ionization, correct boundary conditions are only satisfied in this restricted coordinate space region. Thus, ϕ_β^- presents also a one-target center character and so the CB1 approximation will not give an adequate description of ionized electrons moving close to the projectile in the exit channel. This physical behavior, where the electron travels in the threshold of the continuum of the attractive projectile field is known as electron capture to the continuum (ECC). It must be also mentioned that the application of the active electron Schrödinger equation on the wave function given in Eq. (3) results in

$$(H_\alpha - E_\alpha)\phi_\alpha^+ = V_\alpha\phi_\alpha^+ \tag{5}$$

with the perturbative potential given by

$$V_\alpha = -\frac{Z_P}{s}+\frac{Z_P}{R}. \tag{6}$$

In this expression the second term results from the inclusion, in the initial wave function, of the projectile-active electron interaction at large asymptotic separation between both particles. Thus, only the short range part of this interaction contributes to the perturbative potential. It is easy to show that the corresponding eikonal phases appearing in the initial and final wave functions and depending on $\boldsymbol{R}$ in CB1 may be neglected when cross sections integrated over the projectile scattering angle are considered [18].

Finally, note that in both CDW-EIS and CB1 quantum mechanical calculations, the effective target charge Z_T^* is taken as $Z_T^*=\sqrt{-2n_\alpha^2\varepsilon_\alpha}$ where n_α refers to the principal quantum number of each atomic orbital component used in each molecular orbital

expansion whereas the active electron orbital energy ε_α is related to the ionization energies B_j of the occupied molecular orbitals by $\varepsilon_\alpha = -B_j$. Each molecular orbital is thus described by using a basis of effective atomic ones, as explained in the following.

2.3. The target description

In the present work, the RNA-uracil target is described via its molecular orbitals by employing the quantum chemical GAUSSIAN 03 program [7]. In the latter, the target wave functions are computed at the Hartree–Fock level optimized at the MP2/6–31G(d) computational level, *i.e.* by including correlation calculations at the second order of perturbation theory MP2 and by using GAUSSIAN-type orbitals added to a double-zeta valence shell and polarization orbitals on non-hydrogen atoms. Total-energy calculations are then performed in the gas phase with the Gaussian 09 software at the RHF/3–21G level of theory. The ionization potentials (IP's) calculated at the RHF/3–21G level are in good agreement with the experiments, with in particular a mean absolute error of about 0.16 eV in comparison with the results of Hush and Cheung [8]. Besides, the computed ionization energies of the occupied molecular orbitals of the nucleobase are scaled so that their calculated Koopmans ionization energy *i.e.* the ionization energy of their highest occupied molecular orbital (HOMO) coincides with the experimental value of the ionization potential measured by Hush and Cheung. For each MO, the effective number of electrons relatively to any atomic component is derived from a standard Mulliken population analysis. For more details, we refer the reader to our previous work [3] where all the needed input parameters are reported by means of detailed tables including the population of all the molecular subshells for the DNA/RNA components (bases and sugar–phosphate backbone).

Under these conditions, the total ionization cross section are seen as a linear combination of atomic ones (H_{1s}, C_{1s}, C_{2s}, C_{2p}, N_{1s}, N_{2s}, N_{2p}, O_{1s}, O_{2s}, O_{2p}, P_{1s}, P_{2s}, P_{3s}, P_{2p}, and P_{3p}) weighted by the effective occupation electron number, namely

$$\sigma = \sum_{j=1}^{N} \sigma_j = \sum_{j=1}^{N} \sum_{i}^{N_j} \xi_{j,i} . \sigma_{at,i}, \tag{7}$$

where N refers to the number of molecular orbitals of the impacted bio-molecule (here $N = 39$ for uracil) whereas N_j is the total number of atomic components of the j-molecular orbital and $\sigma_{at,i}$ the corresponding atomic orbital cross sections involved in the present LCAO description.

Let us add that an independent active electron approximation is here employed: it consists in considering the non-ionized *passive* target electrons as frozen in their initial orbitals during the collision process, what is generally assumed to overcome the difficulty of taking into account the dynamical correlation between active and passive electrons in particular for large molecules like those here investigated. Thus, within this approximation, the interaction between the projectile and the passive electrons only affects the trajectory of the incident particle. Consequently, its contribution to the ionization reaction itself is neglected, what is independent of the quantum approximation used for describing the ion-induced ionization process of atoms and molecules, all the more that we here only consider calculations of cross sections integrated over the projectile scattering angle (for more details see [9]).

3. Experimental method

The experimental setup and method have been described elsewhere and for more details we refer the interested reader to Ref. [5]. In brief, a beam of 1 MeV H^+ extracted from a Van de Graff accelerator of Kyoto University was well collimated to about 1×3 mm^2 in size and was introduced into a double mu-metal shielded collision chamber. A typical beam current of about 50 nA measured by a Faraday cup was used in this work. An effusive molecular beam target of uracil was produced by heating crystalline uracil powder (99% purity) in a stainless steel oven at a temperature of 473 K. The energy and angular distributions of secondary electrons ejected from uracil molecules were measured by a 45° parallel plate electrostatic spectrometer. The measurements were carried out for electron energies from 1 eV to 1 keV and emission angles from 15° to 165°. Note that the pressure of the collision chamber was below 2×10^{-7} Torr and the residual magnetic field inside the chamber was less than a few mG. Experimental errors on the obtained single and doubly differential cross sections are 8–13%.

4. Results and discussion

In Fig. 1, we report the theoretical doubly differential ionization cross sections provided by the CB1and the CDW-EIS descriptions, as a function of the ejected electron energies, for an incident proton energy of 1 MeV and for given ejection directions ranging from 15° to 165°.

We clearly observe a very good agreement between the experiments and the theoretical predictions over the whole angular range here investigated, except in the very low angle region where the two sets of theoretical data tend to overestimate the measurements, by a factor of about 2 and 3 for the CDW-EIS and the CB1 results, respectively. The origin of this disagreement is not clear at present. However, it may possibly be attributed to a detector-counting loss of low energy electrons resulting from secondary

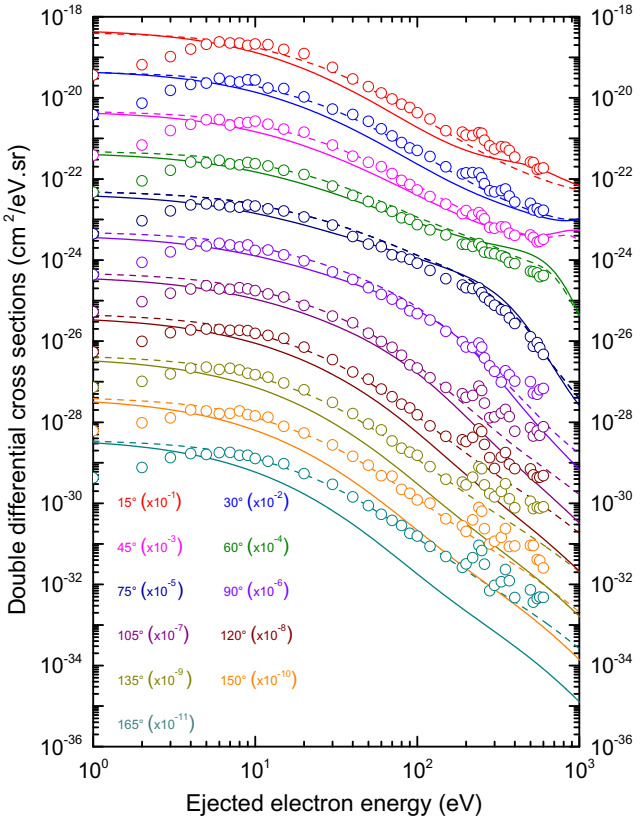

Fig. 1. (Color online) Comparison between experimental and theoretical doubly differential cross sections (CDW-EIS and CB1: solid and dashed line, respectively) for 1 MeV-protons colliding with uracil at different electron emission angles. Multiplicative factors have been used for clarity reasons.

scatterings into other directions from the detector direction during flight inside the polyatomic uracil molecule.

Besides, huge discrepancies may be observed between the CDW-EIS results and the experimental data in the backward scattering region at large electron emission energies, a characteristic behavior of the CDW-EIS model. This behavior is matter of present research. For atomic targets, backward emission at high energies is produced through a two step process where the active electron suffers a first interaction with the projectile, acquiring its high velocity, penetrating then the residual electron cloud and scattering almost elastically in a close encounter with the target nucleus [9]. This mechanism can be partially taken into account if the dynamical screening produced by the electrons remaining bound to the target on the ionized one (for more details we refer the reader to the work of Monti et al. [19]) is considered in the calculations. However, some discrepancy still exists and it could come perhaps from the inclusion, at intermediate collision times, of the electron-projectile continuum in the description of the exit channel, which is also considered in the CB1 approximation but only at infinite separation between the aggregates of the total collision system. It must be noted that it is important to take into account the attractive action of the projectile field in the exit channel to obtain a correct representation of electron emission in the forward direction (in particular to describe structures associated with the ECC mechanism) but perhaps its inclusion overestimates its real influence for backward emission, reducing thus the resulting spectrum at large ejection angles. Thus, the two-centre model appears as necessary to describe the spectrum of ejected electrons as it is determined as a function of their final energy, at fixed forward emission angles [9]. The one-centre CB1 will be not valid under these kinematical conditions. A possible way to eliminate the inadequate behavior of CDW-EIS at backward emission is through the use of dynamical target charges instead of the effective ones here employed, in order to preserve the good predictions of CDW-EIS for forward emission and the ones of CB1 for ionization at large angles.

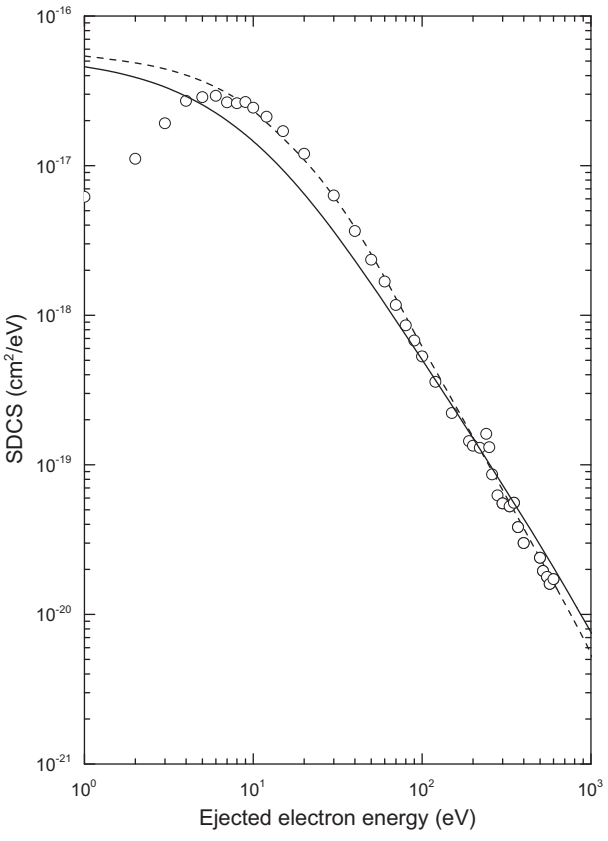

Fig. 2. Comparison between experimental and theoretical singly differential cross sections (CDW-EIS and CB1: solid and dashed line, respectively) for 1 MeV-protons colliding with uracil.

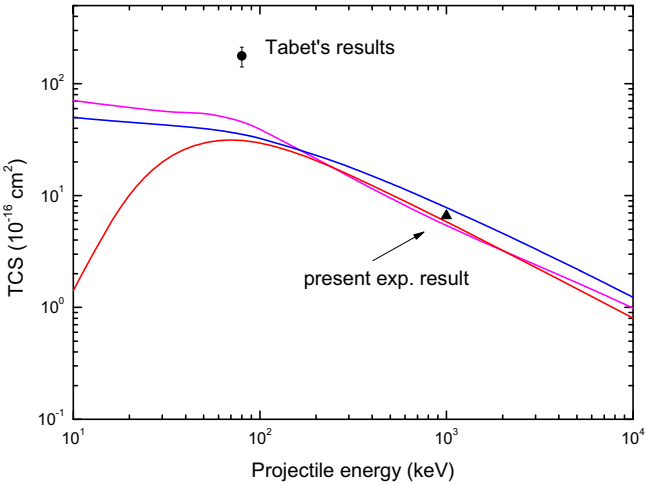

Fig. 3. (Color online) Comparison between experimental and theoretical total cross sections: CDW-EIS (red line), CB1 (blue line) and CTMC-COB (magenta line) for protons colliding with uracil. (For interpretation of the references to colour in this figure legend, the reader is referred to the web version of this article.)

In Fig. 2, CDW-EIS and CB1 SDCS for uracil impacted by 1 MeV-protons are reported and compared with measurements. Here again, the agreement between theory and experiments is very good provided that the ejected energies are larger than 10 eV (for the CB1 model) and 100 eV (for the CDW-EIS one).

Finally, by integrating both the experimental and the theoretical singly differential cross sections we get the total ionization cross sections of uracil which are reported in Fig. 3 and compared to previous classical calculations performed within the Classical Trajectory-Monte Carlo-Classical Over Barrier (CTMC-COB) framework [20] as well as experimental data provided by Tabet et al. [21] for 80 keV-protons. A good agreement may be observed between the CDW-EIS and the CB1 theoretical predictions and the present experimental data whereas a large difference is reported with the Tabet's [21] measurement.

5. Conclusions

In the present work, single ionization of RNA-uracil by 1 MeV-proton impact has been both experimentally and theoretically investigated. A brief description of the experimental apparatus as well as the quantum mechanical theories has been reported.

An experiment/theory confrontation of the doubly differential cross sections has then clearly pointed out a theoretical overestimation of the measurements for ejection energies lower than about 10 eV. As for the CDW-EIS model, it has shown its limitation for predicting the angular distribution of the secondary electrons for ejection angles greater than about 120° contrary to the CB1 model which reproduces very well the experimental observations.

Similarly, CB1 singly differential cross sections were found in very good agreement with the experimental data provided that the ejection energies was greater than about 10 eV while the CDW-EIS results have shown a systematic underestimation until about 100 eV. Finally, the experimental total ionization cross section of RNA-uracil at 1 MeV-proton impact has been compared to the present theoretical predictions and shown a reasonable agreement. However, in comparison to the only other existing experimental measurement – for an impact energy of 80 keV – the

present models have clearly pointed out a huge discrepancy. In this context, additional accurate measurements are definitely needed in order to further validate the here proposed theoretical models.

Acknowledgments

This work has been developed as part of the activities planned in the Programme de Coopération ECOS-*Sud* A09E04 as well as in the project PICS 5921 (THEOS) of the Centre National de la Recherche Scientifique, the project PICT 2145 of the Agencia Nacional de Promoción Científica y Tecnológica and the projects PIP 1026 and PIP 0033 from CONICET.

References

[1] L.H. Toburen, Challenges in Monte Carlo track structure modeling, Int. J. Radiat. Biol. 88 (2011) 2–9.
[2] C. Champion, J. Hanssen, R.D. Rivarola, The first born approximation for ionization and charge transfer in energetic collision of multiply charged ions in matter, Book Series: Advances in Quantum Chemistry, in press.
[3] M.E. Galassi, C. Champion, P.F. Weck, R.D. Rivarola, O. Fojón, J. Hanssen, Quantum-mechanical predictions of DNA and RNA ionization by energetic proton beams, Phys. Med. Biol. 57 (2012) 2081–2099.
[4] C. Champion, P.F. Weck, H. Lekadir, M.E. Galassi, O. Fojón, P. Abufager, R.D. Rivarola, J. Hanssen, Proton-induced single electron capture on DNA/RNA bases, Phys. Med. Biol 57 (2012) 3039–3049.
[5] Y. Iriki, Y. Kikuchi, M. Imai, A. Itoh, Absolute doubly differential cross sections for ionization of adenine by 1.0-MeV protons, Phys. Rev. A 84 (2011) 032704.
[6] Y. Iriki, Y. Kikuchi, M. Imai, A. Itoh, Proton-impact ionization cross sections of adenine measured at 0.5 and 2.0 MeV by electron spectroscopy, Phys. Rev. A 84 (2011) 052719.
[7] M.J. Frisch et al., Gaussian 09, Revision A.02, Gaussian Inc., Wallingford CT, 2009.
[8] N.S. Hush, A. Cheung, Ionization potentials and donor properties of nucleic acid bases and related compounds, Chem. Phys. Lett. 34 (1975) 11.
[9] N. Stolterfoht, R. DuBois, R.D. Rivarola, In Electron Emission in Heavy Ion-atom Collisions, Springer, Berlin, 1997.
[10] P.D. Fainstein, V.H. Ponce, R.D. Rivarola, A theoretical model for ionization in ion-atom collisions. Application for the impact of multicharged projectiles on helium, J. Phys. B At. Mol. Opt. Phys. 21 (1988) 287.
[11] P.D. Fainstein, V.H. Ponce, R.D. Rivarola, Two-centre effects in ionization by ion impact, J. Phys. B At. Mol. Opt. Phys. 24 (1991) 3091.
[12] R. Gayet, Charge exchange scattering amplitude to first order of a three body expansion, J. Phys. B 5 (1972) 483.
[13] Dž. Belkić, A quantum theory of ionization in fast collisions between ions and atomic systems, J. Phys. B 11 (1978) 3529.
[14] D.S.F. Crothers, J.F. McCann, Ionisation of atoms by ion impact, J. Phys. B 16 (1983) 3229.
[15] D.P. Dewangan, J. Eichler, Boundary conditions and the strong potential Born approximation for electron capture, J. Phys. B 18 (1985) L65.
[16] Dž. Belkić, R. Gayet, J. Hanssen, A. Salin, The first Born approximation for charge transfer collisions, J. Phys. B 19 (1986) 2945.
[17] Tachino C 2011, Ph.D. Thesis, Single and Multiple Ionization in Diatomic Molecules, Universidad Nacional de Rosario, unpublished.
[18] C. Champion, M.E. Galassi, P.F. Weck, O. Fojón, J. Hanssen, R.D. Rivarola, Quantum-mechanical contributions to numerical simulations of charged particle transport at the DNA scale in Radiation damage in biomolecular systems, in: G.G. Garcia Gomez-Tejedor, M.C. Fuss (Eds.), Springer, 2012, p. 263 (Chapter 16).
[19] J.M. Monti, O.A. Fojón, J. Hanssen, R.D. Rivarola, Influence of the dynamic screening on single-electron ionization of multi-electron atoms, J. Phys. B At. Mol. Opt. Phys. 43 (2010) 205203.
[20] H. Lekadir, I. Abbas, C. Champion, O. Fojón, R.D. Rivarola, J. Hanssen, Single electron loss cross sections of DNA/RNA bases impacted by energetic multi-charge ions: a classical Monte Carlo approach, Phys. Rev. A 79 (2009) 062710.
[21] J. Tabet, S. Eden, S. Feil, H. Abdoul-Carime, B. Farizon, M. Farizon, S. Ouaskit, T.D. Märk, Absolute total and partial cross sections for ionization of nucleobases by proton impact in the Bragg peak velocity range, Phys. Rev. A 82 (2010) 022703.